

Spectral decoding in fiber-optic interferometric sensors

MACIEJ WITCZYŃSKI, MONIKA BORWIŃSKA, IWONA JASTRZEBSKA

Institute of Physics, Wrocław University of Technology, Wybrzeże Wyspiańskiego 27, 50–370 Wrocław, Poland.

Principles of white-light interferometric techniques are described in this paper. Different spectral decoding methods applied to low coherence interferometry are also presented. Among them one can distinguish: direct recovering of an optical path difference with use of second interferometer as a spectrum analyzing device, several wavelength interrogation with use of a spectrometer or suitable narrow-band optical filters, and chromatic monitoring in a wider spectrum. The last decoding method was applied to test the performance of fiber optic interferometric pressure and temperature sensors. A diffraction grating was used to monitor a wide part of the output spectrum. The phase shift induced by measurand changes in both sensors was determined with a fringe counting method.

1. Introduction

In recent years, the optical fiber sensor technology is becoming more and more popular. Especially interferometric sensors are of great interest since they offer high resolution of measurements and large dynamic range [1]. Within fiber optic interferometric sensors, these employing broadband spectral sources gain much attention due to their many advantages like possibility of unambiguous measurements, coherent noise reduction and coherency multiplexing. The sensing method often called “white-light” or “low-coherence” interferometry was first reported in 1983 [2]. At the beginning of the paper the principles of white-light interferometry are presented. In general, changes of the optical path difference in white-light interferometric sensors induced by external parameters can be detected by two methods: spectral domain decoding and phase domain decoding. In this article, the spectral decoding methods are carefully reviewed. Among them one can distinguish the following: interferometer/interferometer configuration with direct recovering of the optical path difference, monitoring of several wavelengths and chromatic monitoring in a wider spectrum. At the end, the authors present preliminary testing of a temperature sensor based on a Fabry–Perot (F–P) interferometer and a pressure sensor employing a “side-hole” fiber. The experimental data obtained using a spectral decoding method were used to retrieve the information about the optical phase. It was noticed that changes of a cosine fringe pattern in spectral domain can be easily and in a simple way transferred to the value of the optical path difference.

2. Principles of fiber-optic white-light interferometric sensors

The general structure of a fiber-optic sensor consists of an optical source, optical fibers, an element modulating an optical signal according to changes of a measurand, an optical detector and processing electronics (Fig. 1). The final signal, which is the output signal of the electronic block V_0 , depends upon the optical properties of each system part. Thus, the general sensor response depends on the light modulation introduced by measurand but also on many additional factors which must be taken into account when results are interpreted. In general, the modulation of an optical signal caused by the measurand can concern phase, polarization or intensity. In multimode fiber sensors, the only parameter of the light wave which can be conserved is intensity. In this case, the output signal of the sensor depends on the delivered light intensity and its distribution in the wavelength domain. The measurand can modulate the spectral distribution of light intensity due to different phenomena: wavelength dependent absorption, luminescence, dispersion, scattering and interference. The last one relies upon producing optical interference in polychromatic light and is based on the fact that the condition for destructive interference cannot be fulfilled simultaneously for all wavelengths. Therefore the wavelengths corresponding to the destructive interference are shifted within the source spectrum when the optical path difference changes. Since the optical path difference depends upon the refractive index and the geometrical path difference, it offers the possibility of monitoring mass density or displacement caused, for example, by pressure or temperature. In practice, the interference in polychromatic light is utilized in sensors named white-light interferometric sensors.

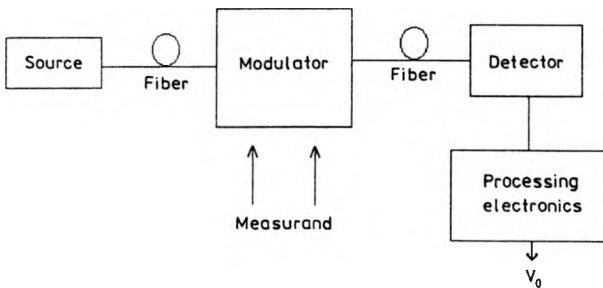


Fig. 1. Structure of a multimode fiber sensor system.

The most basic fiber-optic sensor configuration used for white-light interferometry is shown schematically in Fig. 2. Light from a broadband source L is transmitted to the interferometric sensor S via a directional coupler and a fiber optic link. At the sensor input the amplitude of the light E_0 is divided into two components, E_1 and E_2 , which interfere with each other at the sensor output. The optical path difference δ between them depends upon the value of measurand. The output of the sensor is coupled to an optical processor P that consists of a second optical system necessary to extract information about the optical path difference.

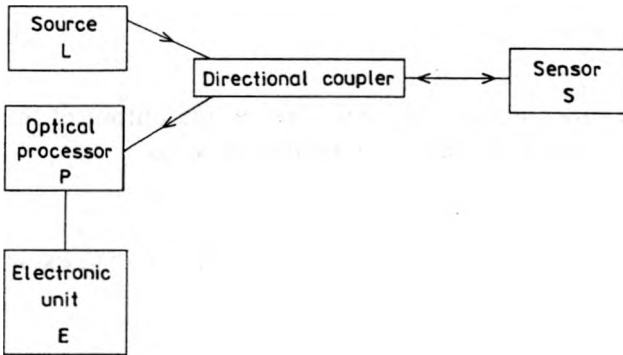


Fig. 2. Basic elements of a fiber-optic white-light interferometric sensor.

The processing system can take one of the two forms: it can be a spectrometer or second interferometer (called the decoding interferometer). At the output of the processing system there is an electronic unit E with a photodetector, which generates an analog electrical signal proportional to the value of optical path difference, and hence to the value of measurand [1], [2].

In the analysis of the polychromatic interference which takes place in a two beam sensing interferometer, one can represent the output beams of a given frequency ω in the following way:

$$\begin{aligned} E_1(\omega) &= A_1(\omega) \exp i L_1 \beta(\omega), \\ E_2(\omega) &= A_2(\omega) \exp i L_2 \beta(\omega) \end{aligned} \quad (1)$$

where $A_1(\omega)$ and $A_2(\omega)$ are amplitudes of the beams, L_1 and L_2 are the lengths of the first and second arm of the interferometer and $\beta(\omega)$ is a propagation constant.

The propagation constant in dispersive medium for a given frequency ω is expressed by

$$\beta(\omega) = \frac{2\pi n(\omega)}{\lambda} = \frac{1}{c_0} \omega n(\omega) \quad (2)$$

where λ is the wavelength, c_0 is the light speed. The propagation constant is then dispersion quantity that can be developed in Taylor series around frequency ω_0

$$\beta(\omega) = \beta(\omega_0) + \frac{d\beta}{d\omega}(\omega - \omega_0) + \dots \quad (3)$$

To obtain a more convenient expression for $\beta(\omega)$ it is necessary to differentiate Eq. (2)

$$\frac{d\beta}{d\omega} = \frac{1}{c_0} \left[n(\lambda_0) - \lambda \frac{dn}{d\lambda} \right] = \frac{N(\omega_0)}{c_0} \quad (4)$$

where $N(\omega)$ is the group refractive index. When expression (4) is inserted into Eq. (3), we obtain the final form of the propagation constant

$$\beta(\omega) = \beta(\omega_0) + \frac{N(\omega_0)}{c_0}(\omega - \omega_0). \quad (5)$$

The two beams $E_1(\omega)$ and $E_2(\omega)$ superimpose with each other at the output of the interferometer. The resultant complex amplitude can be expressed as

$$E(\omega) = E_1(\omega) + E_2(\omega). \quad (6)$$

The output amplitudes $E_1(\omega)$ and $E_2(\omega)$ are also influenced by transmission coefficients:

$$\begin{aligned} E_1(\omega) &= A_0(\omega)t_1(\omega)\exp iL_1\beta(\omega), \\ E_2(\omega) &= A_0(\omega)t_2(\omega)\exp iL_2\beta(\omega) \end{aligned} \quad (7)$$

where $t_1(\omega)$ and $t_2(\omega)$ are the spectral transmission coefficients related to the respective arms of the interferometer and $A_0(\omega)$ is the amplitude of the light wave at the input of the interferometer for a frequency ω . According to Eq. (6), the spectral intensity of the light wave at the output is

$$I_s(\omega) = |E_1(\omega) + E_2(\omega)|^2 = |E_1(\omega)|^2 + |E_2(\omega)|^2 + 2\text{Re}\{E_1(\omega)E_2^*(\omega)\}, \quad (8)$$

which can also be written as

$$I_s(\omega) = A_0(\omega)^2[|t_1(\omega)|^2 + |t_2(\omega)|^2] + 2\text{Re}[A_0(\omega)^2 t_1(\omega)t_2^*(\omega)\exp i\beta(\omega)\Delta L] \quad (9)$$

where $\Delta L = L_1 - L_2$ is the geometrical path difference. After certain transformations one can obtain a final expression for spectral intensity at the output of the interferometer

$$I_s(\omega) = I_0(\omega) \left[1 + c(\omega) \cos\left(\frac{2\pi n(\omega)\Delta L}{\lambda}\right) \right] \quad (10)$$

where

$$I_0(\omega) = A_0(\omega)^2[|t_1(\omega)|^2 + |t_2(\omega)|^2] \quad (11)$$

is the spectral intensity distribution depending upon the source spectrum and the spectral transmission coefficients of the interferometer and $c(\omega)$ is a contrast function that differs with respect to the frequency of the light and is given by

$$c(\omega) = 2 \frac{|t_1(\omega)t_2(\omega)|}{|t_1(\omega)|^2 + |t_2(\omega)|^2}. \quad (12)$$

Integration of Eq. (9) over frequency gives the total light intensity at the output of the interferometer

$$I = \int_0^{\infty} I_s(\omega) d\omega. \quad (13)$$

The integral of the first component of Eq. (9) is

$$I_0 = \int_0^{\infty} A_0(\omega)^2 (|t_1(\omega)|^2 + |t_2(\omega)|^2) d\omega. \quad (14)$$

Using the expression for $\beta(\omega)$ from Eq. (5) and changing the variable from ω to $(\omega - \omega_0)$, one can integrate the second component of Eq. (9) in the following way:

$$\begin{aligned} & 2\text{Re} \int_0^{\infty} A_0(\omega)^2 t_1(\omega) t_2^*(\omega) \exp[i\beta(\omega)\Delta L] d\omega \\ &= 2\text{Re} \left\{ \exp[i\beta(\omega_0)\Delta L] \int_0^{\infty} |A_0(\omega)|^2 t_1(\omega - \omega_0) t_2^*(\omega - \omega_0) \right. \\ & \quad \times \exp \left[i \frac{N(\omega_0)}{c_0} \Delta L (\omega - \omega_0) \right] d(\omega - \omega_0) \left. \right\} \\ &= 2\text{Re} \left\{ \exp[i\beta(\omega_0)\Delta L] \frac{I_0}{2} c \left(\frac{N(\omega_0)}{c_0} \Delta L \right) \right\} \end{aligned} \quad (15)$$

where

$$c \left(\frac{N(\omega_0)}{c_0} \Delta L \right) = \frac{2}{I_0} \mathcal{F} \{ |A_0(\omega)|^2 t_1(\omega) t_2^*(\omega) \} \quad (16)$$

is the Fourier transform of the function: $\{|A_0(\omega)|^2 t_1(\omega) t_2^*(\omega)\}$ multiplied by $2/I_0$ and represents the envelope of the interference pattern. Thus, finally, from Eqs. (13)–(16) the total intensity transmitted by the interferometer is

$$I = I_0 + I_0 c \left(\frac{N(\omega_0)}{c_0} \Delta L \right) \cos(\beta(\omega_0)\Delta L), \quad (17)$$

which can also be written as

$$I(\delta) = I_0 \left[1 + c(\tau) \cos \left(\frac{2\pi}{\lambda_0} \delta \right) \right] \quad (18)$$

where I_0 is the average output intensity, δ is the optical path difference between the interfering beams ($\delta = n\Delta L$) and $c(\tau)$ is the contrast function depending upon the time delay $\tau = N\Delta L/c_0$ (for non-dispersive media $\tau = \delta/c_0$) of the interferometer.

The essence of white-light interferometry consists in using spectrally broadband instead of narrow-band source, which makes it possible to extend the range of unambiguous (*i.e.*, absolute) measurements of the optical phase difference from a single to many interference fringes. This can be done due to the fact that cosine fringes are modulated by the contrast function, which enables the determination of fringe order in non-dispersive medium. In the case of narrow-band source the contrast function is equal approximately to unity over many fringes and the unambiguous range of measurements is limited to a single fringe [1]. Another situation is when polychromatic light propagates in a dispersive medium, for example, in a fiber optic interferometer. Then, according to Eq. (17), positions of fringes in the interference pattern depend upon the phase optical path difference $n\Delta L$ and the position of the pattern envelope depends upon the group optical path difference $N\Delta L$.

Equation (18) relates to the situation in which the group optical path difference ($c_0\tau$) between the two interfering beams is less than the coherence length ($c_0\tau_c$, where τ_c is the correlation time). Then interference effects occur in the spatial domain. When the path difference is greater than the coherence length, it is not possible to observe interference in the spatial domain, and it can be detected in the spectral domain [3], [4]. In this case, the interference pattern is described by Eq. (10) which can also be written after the change of the variable $\sigma = \omega/2\pi c_0$ as

$$I(\sigma) = I_0(\sigma)[1 + c(\sigma)\cos(2\pi\sigma\delta)] \quad (19)$$

where $\sigma = 1/\lambda$ is the wave number and δ is the optical path difference. As can be seen from Eq. (19), the spectral transmission varies sinusoidally with wave number.

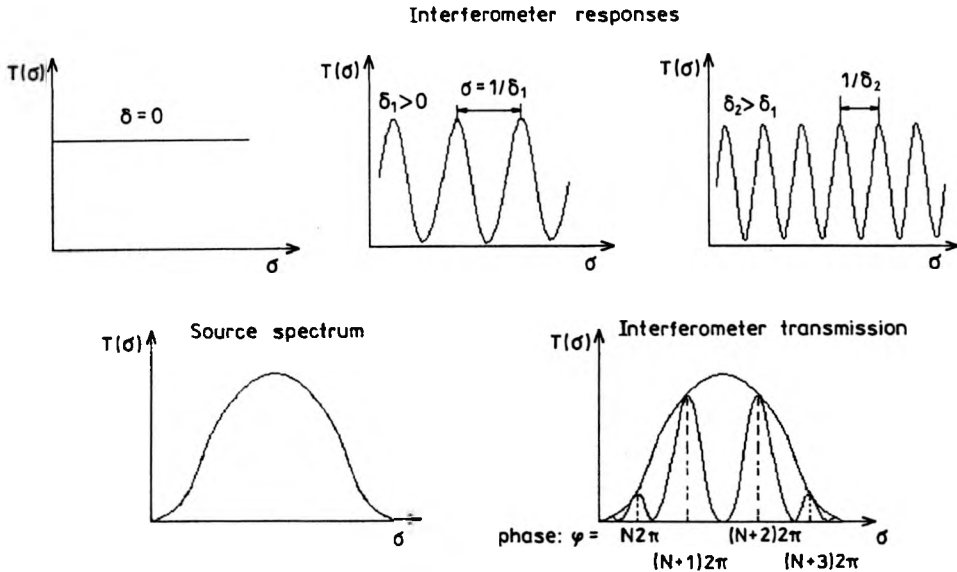


Fig. 3. Spectral modulation of a two-beam interferometer.

The frequency of this spectral modulation is proportional to the path difference δ , which is shown schematically in Fig. 3. One can notice that for $\delta = 0$ there is no spectral modulation and the interferometer is transparent for all wavelengths. If the path difference δ varies from zero, the function takes the form of cosine curve with peaks at the points where $\sigma\delta = N$, with N being an integer number indicating fringe order. Therefore, the spacing of adjacent transmission peaks is proportional to the inverse of the path difference ($\sigma \sim 1/\delta$). The output spectrum of the interferometer is the source spectrum modified by the transmission function of the interferometer.

3. Review of spectral decoding methods applied to white-light interferometric sensors

There are two fundamental decoding schemes for white-light interferometry: phase and spectral domain decoding. In the case of the latter, a spectrum analyzing device must be used as the optical processing element P . When this element is an interferometer, it is not possible to get an exact information about spectral intensity distribution. Then the measurement consists first in finding the state when the transmission functions of both interferometers match with each other and next simply retrieving a measurand value in the decoding interferometer. In this procedure there is no explicit analysis of the spectrum. When the processing element is a spectrometer, then a detailed spectral information is obtained which needs subsequent mathematical analysis to reveal information about optical path difference. Another solution is monitoring only a few (usually two or three) single wavelengths using two individual detectors and narrow-band optical filters. All these possibilities are explained in the following examples.

3.1. Interferometer/interferometer configuration with direct recovering of the path difference

This type of sensors is based on two interferometers: a sensing interferometer and a decoding interferometer. The optical path difference in the first one is modulated by the measurand and the path difference in the decoding interferometer varies systematically either in a scanning or in a tracking mode to recover the path difference from the sensing interferometer [5]. An example of such a sensor used for measurements of displacements is shown in Fig. 4. In this case, the system consists of two Michelson interferometers (of course, this type of sensors can also be built with use of other interferometers, *e.g.*, Fabry – Perot), broadband source and an electronic block of feedback which drives one mirror in the receiving interferometer. The

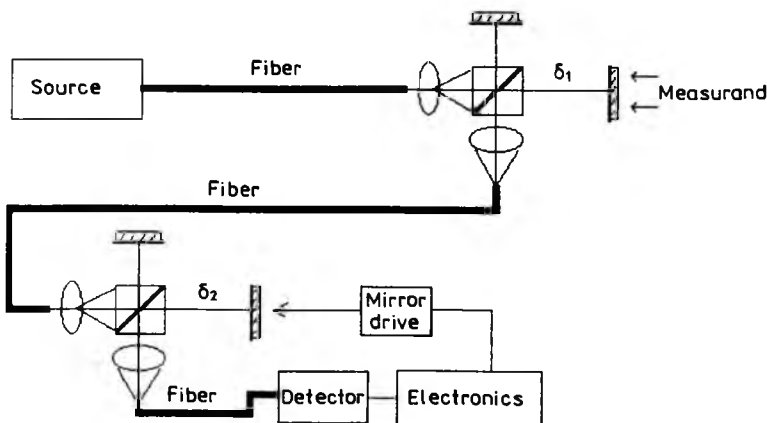


Fig. 4. Example of fiber-optic interferometric sensor for measurements of displacements.

measurand moves one mirror (the displacement of the mirror is ΔL_1) in the sensing interferometer which has the transmission function represented by Eq. (19), thus depending upon the optical path difference ($\delta_1 = 2n\Delta L_1$). In this way, the measurand is encoded into the period of the optical spectrum that is transmitted to the processing interferometer which analyzes this spectrum by changing its path difference ($\delta_2 = 2n\Delta L_2$). Since the transmission function of the second interferometer has the same form as the function of the first interferometer (Eq. (19)), when $\delta_1 = \delta_2$ both functions overlap perfectly and the detected signal is the highest. In this situation, the value of ΔL_1 is reproduced in decoding interferometer, so that $\Delta L_1 = \Delta L_2$ and just by measuring ΔL_2 in a conventional way it is possible to get L_1 . As one can notice in this scheme, the process of decoding spectral information is not connected with many measurements and difficult mathematical operations on the spectra.

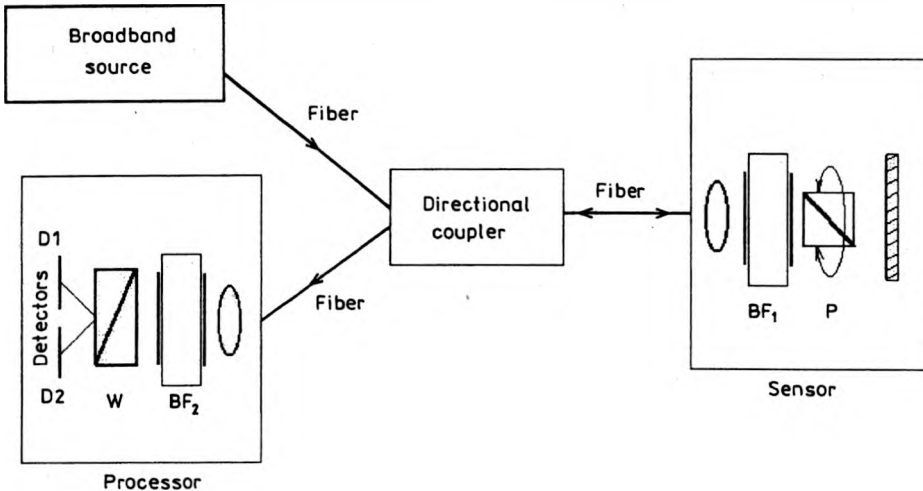


Fig. 5. Fiber-optic rotation sensor employing two interleaved transmission spectra.

Another scheme employing the interferometer/interferometer configuration is the one utilizing interleaved spectra. This design has been used in a sensor for measurement of angular rotations shown in Fig. 5. Here, the light from a broadband source passes through a birefringent F–P filter which transmits only selected wavelengths satisfying resonance condition. A proper selection of the F–P filter thickness BF_1 makes it possible to create two transmission comb spectra shifted with respect to each other by half of a period (interleaved comb spectra). These spectra correspond to the eigenwaves of the filter and therefore they are transmitted along each of the orthogonal birefringent axes of the filter. When the polarizer P from the sensing part has its axis at 45° to the birefringence axis of the F–P filter the intensities of both interleaved spectra are equal to each other. Rotation of the polarizer will alter the relative intensity of these two transmitted spectra. Then the light from the sensing head travels by multimode optical fiber to the decoding part

which consists of a second identical birefringent filter BF_2 and Wollaston prism W that serves as a polarization beam splitting element. Although the multimode fiber mix up the polarization state of the transmitted light, the information about the two orthogonal channel spectra can be recovered due to the fact that the second birefringent filter BF_2 that is at the output of fiber is the same as the first one in the sensing part. Intensities of both orthogonal spectra that are split up by Wollaston prism are measured by detectors, so their relative changes give information about rotation of the polarizer in the sensing head. In general, the presented design of spectral domain processing system is independent of the system losses [2], [5].

3.2. Several wavelength interrogation

One possible way of spectral decoding is the monitoring of several, for instance, two, separate wavelengths using either a spectrometer or two individual detectors and suitable narrow-band optical filters. Usually, the idea is to make one wavelength (reference channel) independent of the modulation, while another one (signal channel) is modulated by the measurand. The ratio of the signals at the two separate wavelengths is then used for referencing against intensity variations. Provided the non-modulated intensity changes are the same for both signal and reference wavelengths, it is possible to achieve an accurate measurement of the modulating parameter. In practice, however, the condition that non-modulated alternations of the intensity are independent of wavelength is very difficult to obtain [1].

Dual wavelength interrogation of low-finesse F–P interferometer is a technique that can be included among the several wavelength monitoring methods. This technique employs passive signal processing based on phase stepping interferometry (PSI) algorithm. A multimode laser diode is used as a light source. Individual modes of the laser are separated in spectral domain by around 0.3 nm [6], and in the case of using the special “hole-burning” effects even by 2–3 nm [7]. Thus, the source of light behaves like two spectrally close but separated narrow-band sources. The light from the laser is coupled via directional coupler into a low-finesse F–P cavity which plays the role of the sensing interferometer. This type of sensors (*i.e.*, Low-Finesse Fiber Fabry–Perot Interferometer – LFFFPI) seems to be very promising for measurements of temperature, pressure, strain and vibrations [6]. The back reflected light is introduced into a monochromator and detected using CCD camera. Another monochromator/CCD arrangement is used to observe a direct laser output from the second arm of directional coupler (Fig. 6), which serves to normalize the intensity detected in the first CCD [6]–[8]. Subsequently the recorded and digitized data is processed in PC. The idea is to recover the interferometric phase of the back reflected light from the F–P interferometer, which thus gives information about the measurand dependent cavity length. Measurements including four separate determination of intensity (two for each wavelength) offer the possibility of calculating the optical phase with the algorithms used in PSI [6], [7]. Recently, an improvement of the presented technique has been reported. The new idea is to make measure-

ments with an increased number of wavelengths using more adjacent modes from the spectrum of the multimode laser diode source (experiments have been carried out with three and four wavelength interrogation [6]).

3.3. Chromatic monitoring in a wider spectrum

Using this approach it is possible to acquire the whole information about the spectrum. In general, the method relies on splitting the optical signal into the spectral components using prism or diffraction grating. The spectrum is then focused onto an array of photodetectors (*e.g.*, CCD). The signal from photodetectors can be numerically processed or displayed onto a chromaticity diagram. This method of spectral decoding is most often used in white-light interferometric sensors applied to surface profiling [9]–[14], precise determination of refractive indices [3], [15] or thickness measurement [3], [16].

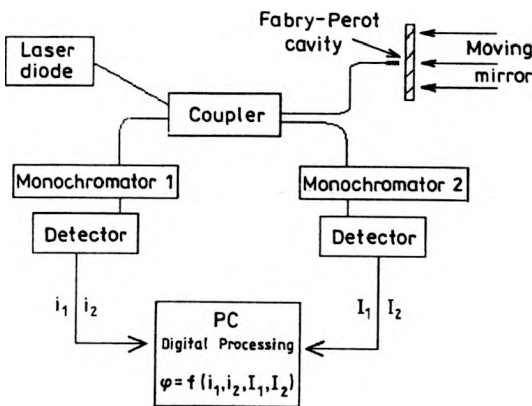


Fig. 6. Interrogation of low finesse Fabry-Perot interferometer using a two wavelength technique.

An example of the spectrally-resolved fiber-optic white-light interferometry sensor used for profilometry is demonstrated in Fig. 6. Here, a broadband source is coupled to Mirau-type interferometric microscope objective [10], [13], which together with the surface of the sample examined creates a sensing interferometer (the sensing interferometer can also be arranged in another way, *e.g.*, Michelson interferometer with the surface of a sample as one of the mirrors). The light from the source is divided by a beam splitter into two beams, which travel along different paths, one of them is reflected on the surface of the sample and the other is reflected on a reference mirror, and then they interfere with each other. At the exit plane of the microscope the white-light interferogram of the surface is collected by an optical fiber. The detection system is a spectroscope. Its entrance slit, placed at the output of the fiber, selects one line of the surface that is profiled (Fig. 7a). The spectroscope separates the spectral components of the light and the CCD camera records a two-dimensional (y, σ) fringe pattern (Fig. 7b), where y is spatial coordinate along the line of the sample which is selected by the entrance slit of the spectroscope and σ is

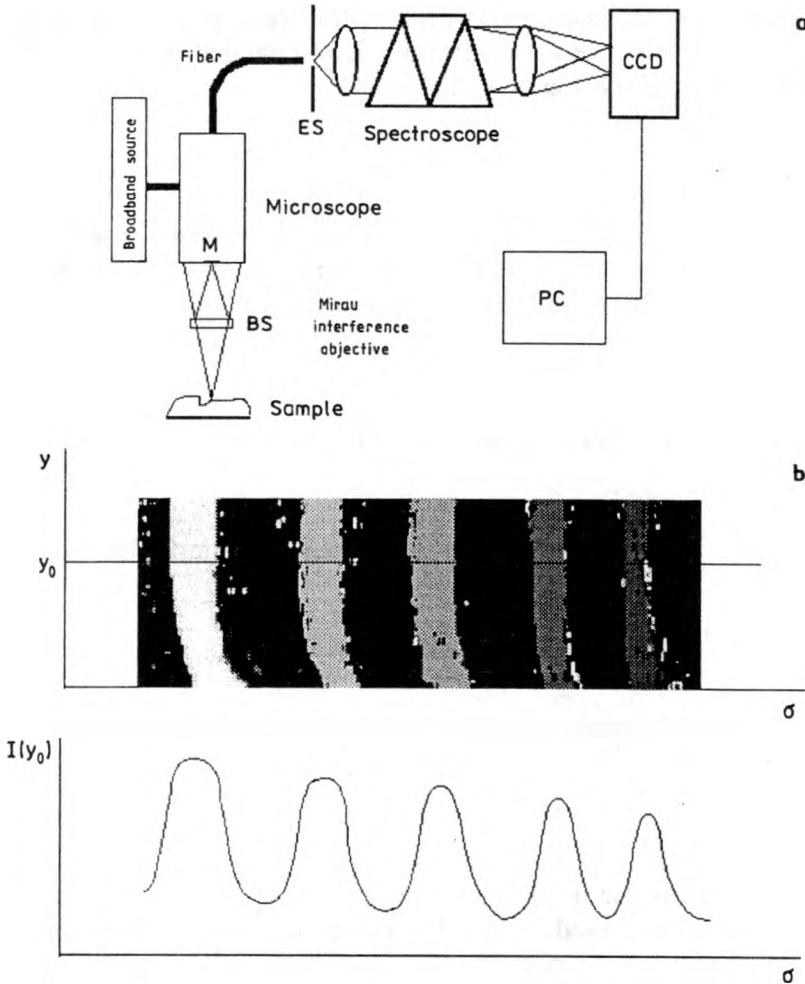


Fig. 7. Example of spectrally-resolved white-light interferometry sensor used as profilometry tool (M – reference mirror, ES – entrance slit, BS – beam splitter) – a. The fringe pattern and the intensity distribution for selected line of this intensity pattern – b.

the wave number. The intensity recorded at a specific point in the interferogram is related to the path difference between two beams according to Eq. (19). This equation is the basis for further treatment of the recorded intensity data, which allows the information about the path difference and hence about the profile of the sample to be retrieved. Different procedures can be used to achieve this goal. One way is the determination of the number of fringes in the interference pattern within a given spectral range [16]. Another way is based on the FFT of fringes in spectral domain [10]. The next solution proposed is based on the analysis of the phase as a function of wave number all over the interference pattern [10], [13].

The evaluation of the phase consists of two steps. In the first step, the phase of the signal is found from intensity measurements at each separated wave number σ through inversion of the cosine function in Eq. (19)

$$\varphi(y, \sigma) = \cos^{-1} \left[\frac{I(\sigma) - I_0}{I_0 \gamma(\sigma)} \right]. \quad (20)$$

These calculations allow us to obtain a linear dependence of the phase φ upon the wave number σ : $\varphi = S\sigma + R$, where S is the linear coefficient of proportionality and R is an irrelevant constant. Since the phase is connected with the optical path difference δ by

$$\varphi(\sigma) = 2\pi\delta\sigma \quad (21)$$

it is easy to achieve from the measurements of S the value of

$$\delta = S/2\pi. \quad (22)$$

This value together with the knowledge of the conditions that are fulfilled at the extrema points

$$\begin{aligned} \sigma_{\max} \delta &= N \quad \text{at every maximum,} \\ \sigma_{\min} \delta &= N + 1/2 \quad \text{at every minimum,} \end{aligned} \quad (23)$$

serve in the second step to determine the fringe order N [10]. This subsequently makes it possible to calculate the absolute phase

$$\varphi_{\text{abs}}(\sigma) = 2N\pi + \varphi(\sigma) \quad (24)$$

and to obtain the exact value of the optical path difference.

Another example of chromatic monitoring method concerns the case where the measured spectral data are represented on two-dimensional colour CIE chromaticity diagrams [1], [17]. A result of interference from a sensing interferometer in the form of white-light interferogram can be detected either with use of spectroscopy/CCD arrangement [17] or by N detectors (N is an integral, in practice usually $N = 2$ or $N = 3$) with different but overlapping spectral responses [1]. The acquired data serves to create the two-dimensional CIE chromaticity diagram which when analyzed gives information about the interferometric path difference [17]. This information is based on the fact noticed by researchers from University of Maryland (USA) that the dominant colour in the progression of colour fringes reverses the direction with which it moves through the visible spectrum when the optical path difference is monotonically increased. This phenomenon can be observed in the $x-y$ CIE chromaticity diagrams as special shapes [17].

4. Experiments

We have tested the performance of two fiber-optic sensors using spectral decoding method. The first one was an intrinsic fiber-optic pressure sensor based on side-hole

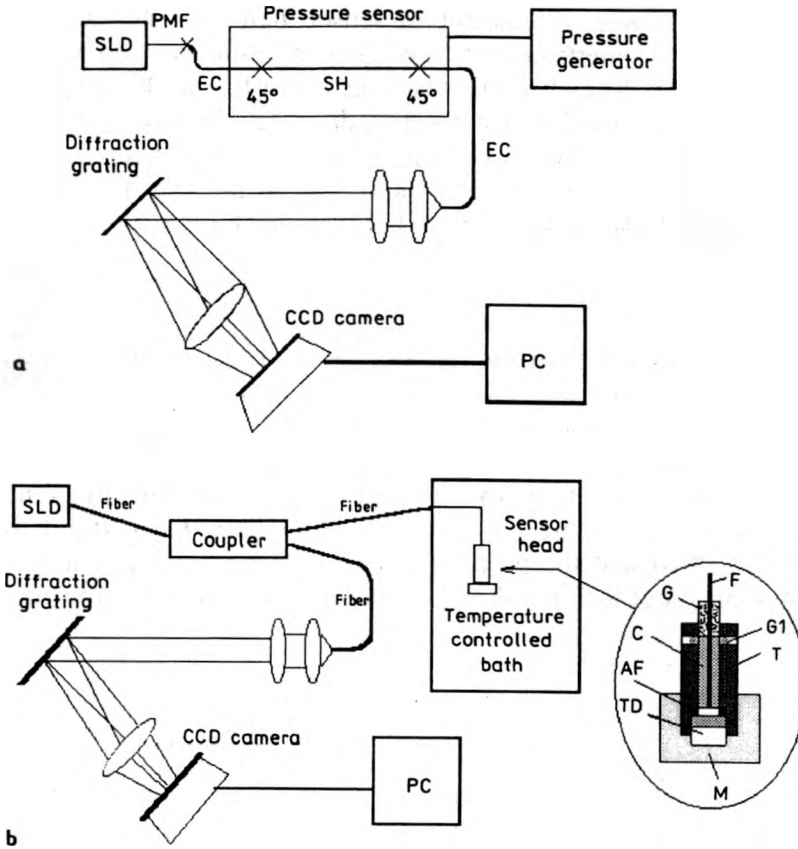


Fig. 8. Experimental setup: a – fiber-optic interferometric pressure sensor (SLD – superluminescent diode, PMF – polarization maintaining fiber, SH – side-hole fiber, EC – elliptical fiber), b – fiber-optic interferometric temperature sensor (F – single-mode fiber, G – gasket, C – glass capillary with the glued fiber, T – aluminium tube, AF – aluminium film, M – mirror, TD – teflon disc, Gl – glue).

fiber (SH). Its construction is shown in Fig. 8a. The light from the broadband source which was a superluminescent diode (SLD, $\lambda_0 = 830 \text{ nm}$, $\Delta\lambda = 15 \text{ nm}$) was delivered to the sensor through a polarization maintaining fiber (PMF). The sensor itself was built up of the highly birefringent side-hole fiber which is very sensitive to pressure. The highly birefringent elliptical core fibers (EC) served as a lead-in and lead-out. They were spliced to sensing fiber with rotation of polarization axes equal to 45° . Due to this fact the two fundamental modes (LP_{01}^x , LP_{01}^y) in the side-hole fiber were equally excited. The sensor relied upon the fact that pressure alterations caused the change of the optical fiber birefringence, which consequently influenced the interference result between two polarization modes at the sensor output. The diffraction grating (1800 lines per mm) allowed the output spectrum to be registered on a CCD camera. The fringe pattern in a spectral domain collected by the CCD camera was digitized, sent to a computer and displayed on a monitor.

The second device tested was a temperature sensor based on F–P interferometer. The cavity of the interferometer was created inside an aluminium tube. A small mirror placed at the end of the tube constituted the totally reflecting surface. Another surface was a partially reflecting layer deposited directly on the end of a single-mode fiber. When temperature was changing the cavity length altered due to the thermal linear expansion of the aluminium tube (Fig. 8b). This effect influenced the interference of the polychromatic light inside the cavity.

5. Results

Examples of the spectral intensity distribution registered at the outputs of the pressure and temperature sensors are shown in Fig. 9. These curves are approximately represented by Eq. (19). Their frequencies depend upon the optical path difference induced by respective sensor. As mentioned above, there are different ways of analyzing such data. One way is to analyze the whole spectrum point by point, which leads to determination of the phase as a function of wavelength $\varphi = f(\lambda)$. This function is then linearly fitted and the proportionality coefficient obtained in this way gives the information about the optical path difference. Another way is to count

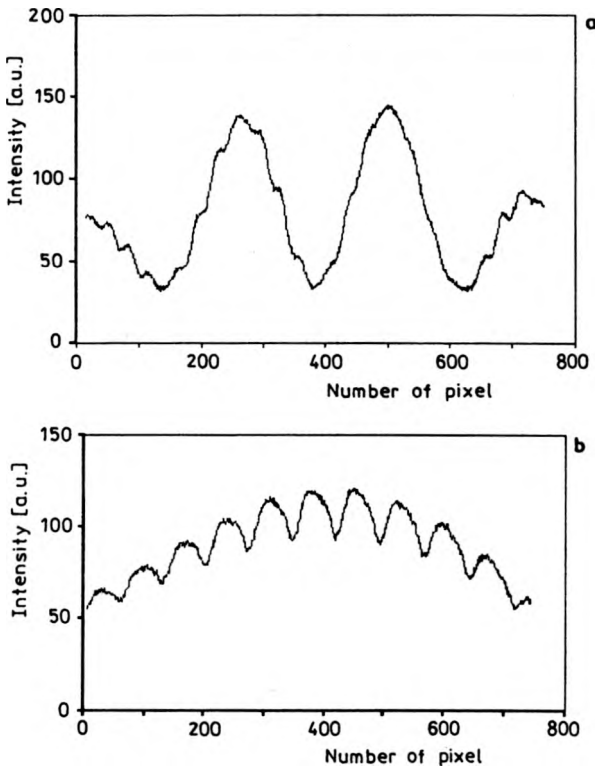


Fig. 9. Spectral intensity distribution registered at the output of the pressure sensor (a) and the temperature sensor (b). The greater number of pixel corresponds to longer wavelength.

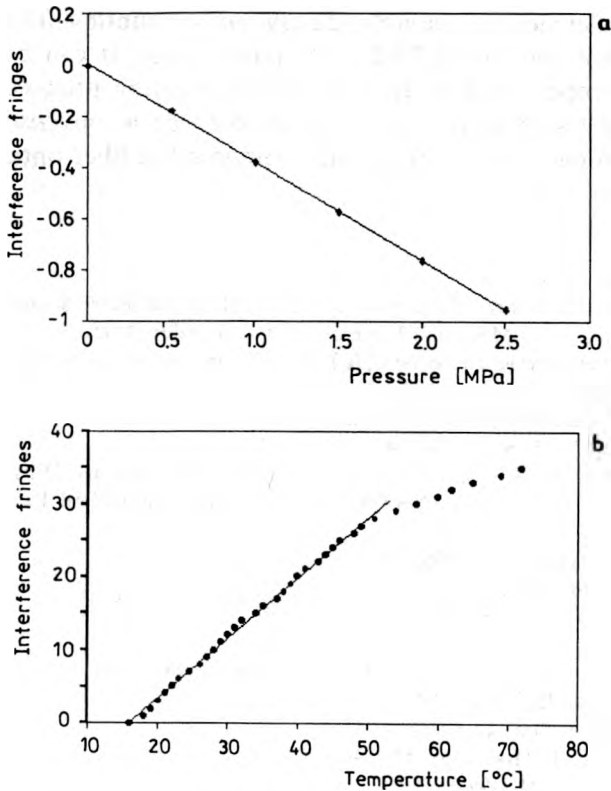


Fig. 10. Displacement of interference fringes induced by measured pressure (a) and temperature (b).

the number of fringes in a certain spectral range (λ_1, λ_2) to establish the frequency of fringes. The method used by the authors to determine the phase shift induced by measurand consisted in counting interference fringes that moved through a given point in the spectrum. The number of fringes that moved can be directly transferred to the phase change or the change of optical path difference ($\varphi = 2\pi N$ and $\delta = \lambda N$, where N is the number of fringes and λ is the wavelength for which the counting was done). An example of diagram showing the number of fringes as a function of pressure changes is depicted in Fig. 10a. A similar function for temperature sensor is shown in Fig. 10b. As can be seen, both responses are linear in a wide range of the measurand value. The nonlinear response of temperature sensor was observed for temperatures higher than 50 °C. This was most probably associated with temperature characteristics of epoxy glue, which was used to fix elements of the F–P resonator.

6. Conclusions

The tests showed that when the spectral decoding scheme is applied to fiber-optic white-light interferometric sensors, a simple and convenient way of retrieving the

information of the optical path difference can be an ordinary fringe counting. The achieved resolution of measurement was about 0.02 interference fringe. It can be further improved by applying a proper software to support the counting process.

The spectral decoding method tested in this work occurred to be a universal method that can be applied to complex measuring systems composed of fiber optic interferometric sensors of different type.

References

- [1] JONES G. R., JONES R. E., JONES R., *Multimode optical fiber sensors*, [In] *Optical Fiber Sensors Technology*, [Eds.] K. T. V. Grattan, B. T. Meggitt, Chapman & Hall, London 1995.
- [2] MEGGITT B. T., *Fiber optic white-light interferometric sensors*, [In] *Optical Fiber Sensors Technology*, [Eds.] K. T. V. Grattan, B. T. Meggitt, Chapman & Hall, London 1995.
- [3] NIRMAL KUMAR V., NARAYANA RAO D., *J. Opt. Soc. Am. B* **12** (1995), 1559.
- [4] NARAYANA RAO D., NIRMAL KUMAR V., *J. Mod. Opt.* **41** (1994), 1757.
- [5] ULRICH R., *Theory of spectral encoding for fiber-optic sensors*, [In] *Optical Fiber Sensors*, [Eds.] A. N. Chester, S. Martellucci, A. M. Verga Scheggi, NATO ASI Series, Martinus Nijhoff Pub., Dordrecht, Boston, Lancaster 1987.
- [6] EZBIRI A., TATAM R. P., *Meas. Sci. Technol.* **7** (1996), 117.
- [7] EZBIRI A., TATAM R. P., *Opt. Lett.* **20** (1995), 1818.
- [8] SANTOS J. L., LEITE A. P., JACKSON D. A., *Appl. Opt.* **31** (1992), 7361.
- [9] CABER P. J., *Appl. Opt.* **32** (1993), 3438.
- [10] CALATRONI J., GUERRERO A., SAINZ C., ESCALONA R., *Opt. Laser Technol.* **28** (1996), 485.
- [11] DE GROOT P., DECK L., *J. Mod. Opt.* **42** (1995), 389.
- [12] HARIHARAN P., MAITREYEE R., *J. Mod. Opt.* **43** (1996), 1797.
- [13] SANDOZ P., TRIBILLON G., PERRIN H., *J. Mod. Opt.* **43** (1996), 701.
- [14] SANDOZ P., TRIBILLON G., *J. Mod. Opt.* **40** (1993), 1691.
- [15] GUERRERO A., SAINZ C., PERRIN H., CASTELL R., CALATRONI J., *Opt. Laser Technol.* **24** (1992), 333.
- [16] GOEDGEBUER J. P., LACOURT A., GUIGNARD M., *Opt. Laser Technol.* **10** (1978), 193.
- [17] KIESS T. E., BERG R. E., *Am. J. Phys.* **64** (1996), 928.

Received February 18, 1999